Atmos. Chem. Phys. Discuss., 3, 1051–1080, 2003
www.atmos-chem-phys.org/acpd/3/1051/

Atmospheric
Chemistry
and Physics
Discussions

Dynamics and chemistry of vortex remnants in late Arctic spring 1997 and 2000: Simulations with the Chemical Lagrangian Model of the Stratosphere (CLaMS)

P. Konopka[1], J.-U. Grooß[1], S. Bausch[1], R. Müller[1], D. S. McKenna[2], O. Morgenstern[3], and Y. Orsolini[4]

[1]Institute for Stratospheric Chemistry (ICG-I), 52425 Jülich, Germany
[2]National Center for Atmospheric Research, Boulder, CO, USA
[3]Max Planck Institut für Meteorologie, Hamburg, Germany
[4]Norwegian Institute for Air Research (NILU), Kjeller, Norway

Received: 30 December 2002 – Accepted: 14 February 2003 – Published: 25 February 2003

Correspondence to: P. Konopka (p.konopka@fz-juelich.de)

Abstract

High resolution simulations of the chemical composition of the Arctic stratosphere during late spring 1997 and 2000 have been conducted with the Chemical Lagrangian Model of the Stratosphere (CLaMS). The simulations were performed for the entire northern hemisphere on two isentropic levels 450 K (≈18 km) and 585 K (≈24 km).

The spatial distribution and the lifetime of the vortex remnants formed after the vortex breakup in May 1997 show a completely different behavior above and below 20 km. Above 20 km, vortex remnants effectively propagate southward (up to 40° N) and are "frozen" in the summer circulation without significant mixing. Below 20 km the southward propagation of the remnants is bounded by the subtropical jet near 55° N. Their lifetime is shorter by a factor of 2 than above 20 km, owing to significant stirring below this altitude. The behavior of vortex remnants formed in March 2000 is similar but, due to an earlier vortex breakup, dominated until mid of May by westerly winds, even above 20 km.

Vortex remnants formed in May 1997 are characterized by large mixing ratios of HCl indicating a negligible contribution of the halogen-induced ozone loss. In contrast, mid-latitude ozone loss in late boreal spring 2000 is dominated by an irreversible transport of the ozone-depleted polar air masses (dilution) and, until mid of April, by halogen-induced ozone destruction within the vortex remnants. By varying the effective diffusivity of CLaMS, the impact of mixing on the formation of $ClONO_2$ and ozone depletion is considered. In particular, the photochemical decomposition of HNO_3 and not mixing with NO_x-rich mid-latitude air is the main source of NO_x within the vortex remnants in March and April 2000. Ozone depletion in the remnants is driven by ClO_x photolytically formed from $ClONO_2$ and can be properly resolved for CLaMS spatial resolution better then 100 km. At 450 K, ozone loss in the vortex remnants contributes by ≈2% to the ozone deficit poleward of 30° N.

1. Introduction

Long-term ground-based measurements over Europe show that the total column of ozone began to decline in the 1970s. The decrease has been greatest in the winter/spring period, with the ozone decline trend in the late 1990s being around 3–6%/decade. The main contribution is located in the 12–20 km altitude range (WMO, 1998).

One of the widely discussed mechanisms contributing to this trend is the ozone depletion in the Arctic vortex and its impact on the mid-latitudes. During winter and spring, chlorine in the polar vortex is activated on the surface of the polar stratospheric clouds and cause severe ozone destruction (WMO, 1998). Knudsen and Grooß (2000) estimated from calculations done for 1995 and 1997, that approximately 40% of the observed TOMS total ozone trends result from the transport of the ozone depleted vortex air into the mid-latitudes. On the other side, using 3d CTM studies Chipperfield and Jones (1999) have shown that during 1990s the dynamical variations dominate the interannual variability of ozone north of 63° with little evidence for a trend towards more wintertime chemical depletion.

The first studies considering the details of the transport of the vortex air into the mid-latitudes were based on LIMS data (LIMS – Limb Infrared Monitor of the Stratosphere) and GCM simulations. Hess (1991) found that long-lived anomalies of tracers were still observed two month after the breakup of the polar vortex in spring 1979. Using the PDF technique for 3d simulations of N_2O, Orsolini (2001) identified some long-lived westward-propagating tracer patterns in the 1998 summer polar stratosphere above 20 km that resulted from the slow advection of coarsely-mixed vortex remnants. Based on 3d CTM simulations with a parameterized ozone chemistry, Piani et al. (2002a) showed that by the end of June, above 420 K, much of the ozone depleted air was transported from the polar regions to the subtropics, whereas below 420 K, these air masses remained polarward of ≈55° N. They suggested that below 420 K the subtropical jet provides an effective transport barrier while stirring after the breakup of the polar vortex is important at upper levels.

Despite these achievements, questions on the lifetime, the spatial distribution, and the year-to-year variability of such remnants are still open. Also their impact on the total ozone column, in particular over the densely populated regions in northern mid-latitudes, needs to be quantified. Furthermore, only few studies exist that discuss the effect of stirring and mixing on the ozone chemistry in the slowly diluting vortex remnants (Marchand et al., 2003).

Inaccurate representation of mixing in photochemical transport models may influence the predictions of stratospheric ozone depletion (Edouard et al., 1996; Searle et al., 1998a,b). Both satellite observations (Riese et al., 1999), in situ measurements (Tuck, 1989), and dynamical model studies based on such experiments (e.g. Plumb et al., 1994; Waugh et al., 1997; Orsolini et al., 1997; Balluch and Haynes, 1997) demonstrated the existence of filamentary structures on a broad range of spatial scales in stratospheric chemical tracer fields. Chemical transport models that do not resolve filamentary structures and do not represent their dissipation times realistically, will not simulate non-linear chemical reactions accurately. Using a photochemical box model to study the impact of mixing on the deactivation of the stratospheric chlorine, (Tan et al., 1998) showed that both box models without mixing and the currently employed grid-based numerical models can, in certain circumstances, significantly over- and underestimate the observed ozone loss rates. Furthermore, based on idealized isentropic simulations, they concluded that a spatial resolution better than 40 km is necessary to obtain a correct description of ozone loss that is not sensitive to the numerical diffusivity of the model.

To study the impact of transport on the spatial distribution, the lifetime, and the ozone chemistry in the vortex remnants in spring/summer 1997 and 2000, we use the high resolution, isentropic (2d) version of the Chemical Lagrangian Model of the Stratosphere (CLaMS) (McKenna et al., 2002b,a). We choose these two periods because of their completely different characteristics with respect to the lifetime of the Arctic polar vortex: Whereas the vortex in 1997 was extremely long-lived with the final breakup around mid-May (Coy et al., 1997), the vortex decay in mid-March 2000 is more typical for the final warmings observed in the last twenty years (Manney and Sabutis, 2000).

The Lagrangian view of transport allows to describe mixing in its own way: Mixing in CLaMS is induced by an adaptive regridding of the (isentropic) air parcels (APs) with mean distance to the next neighbors given by r_0 (model resolution). The regridding procedure is applied after each advection time step Δt (6–24 h) that is conducted in terms of isentropic (2d) trajectories. The mixing intensity is driven by the horizontal deformations in the flow measured by the finite time Lyapunov exponent λ. Significant mixing occurs only in flow regions where λ exceeds a prescribed critical value λ_c. In contrast, in the Eulerian approach the numerical diffusion is always and everywhere present due to the high frequency of interpolations of fluid elements on the fixed spatial grid (Courant criterion), the contribution of the CLaMS reggriding procedure to the transport can be contolled. It can be continuously reduced (e.g. by increasing the critical Lyapunov exponent λ_c) until tracers are solely transported along trajectories without any mass exchange between the APs. We call this (reversible) part of transport pure advection. The regridding procedure is controlled by the critical Lyapunov exponent λ_c, the model resolution r_0, and the length of the advection time step Δt (or the grid adaptation frequency $1/\Delta t$). These parameters define the (irreversible) part of transport, i.e. mixing.

The paper is organized as follows: In Sect. 2 we describe the model configuration and justify the isentropic approximation by comparison of the CLaMS CH_4-distributions with HALOE observations. Section 3 discusses the spatial distribution and the lifetime of the vortex remnants observed in spring and summer 1997 and 2000. In Sect. 4, the ozone-chemistry occurring in these remnants is considered. The impact of mixing on the chlorine deactivation and the ozone loss is discussed in Sect. 5. Finally, conclusions are drawn in Sect. 6.

2. Simulations with CLaMS

Isentropic CLaMS studies are carried out for two periods: 10 April – 31 July 1997 and 10 February – 01 June 2000, at the two isentropic levels 450 and 585 K. The meteorological fields are taken from ECMWF data. As a reference case, we employ a (quasi-uniform) distribution of APs over the northern hemisphere with the distance between the neighboring APs $r_0 = 65$ km and $r_0 = 200$ km north- and southward of 30° N, respectively. The critical Lyapunov exponent λ_c and the time step Δt are set to 1.2 day^{-1} and 24 h, respectively. In the following, we call this configuration of mixing parameters adjusted mixing. The adjusted mixing leads to the best agreement between the CLaMS simulations and the in situ aircraft measurements of tracers observed at the edge of the northern polar vortex during the SOLVE/THESEO-2000 campaign (Konopka et al., 2003). The used combinations of the mixing parameters can be quantified by the so-called effective diffusivity (perpendicular to the wind direction) given as $D_-^c \approx r_0^2/(4\Delta t)\exp(-2\lambda_c\Delta t)$ (McKenna et al., 2002b). For the adjusted mixing D_-^c amounts to 1.1 10^3 m^{2}s^{-1}.

In addition, to study the influence of mixing on chemistry, we consider distributions of APs with spatial resolutions $r_0 = 100$, 200 and 400 km northward of 30° N. The strongest impact on mixing can be achieved by varying the spatial resolution due to the quadratic dependence of the effective diffusivity on r_0. Thus, the corresponding effective diffusivities are 2.6 10^3, 1.1 10^5 and 4.2 10^5 m^{2}s^{-1}. The CLaMS transport scheme resolves horizontal structures up to the order of $r_0 \exp(-\lambda_c \Delta t)$, i.e. for $r_0 = 65$ km the smallest resolved scales are approximately 20 km.

The initial distribution of all chemical species at 10.04.1997 is derived from MLS and HALOE observations using trajectory mapping, tracer/tracer and tracer/equivalent latitude correlations. In addition, ER-2, POAM and TRIPLE observations are taken into account for the initialization at 10.02.2000. The remaining species are initialized from a 2D model climatology. The denitrification in 1997 is derived from the MLS data, whereas a one month temperature history is used for appropriate HNO_3 mixing ratios in February 2000 (Grooß et al., 2002; Konopka et al., 2003).

In Fig. 1 the isentropic CLaMS distributions of CH_4 at 450 and 585 K about 12 days after the vortex breakup in 1997 are shown. For comparison HALOE observations are overlayed (circles). Vortex remnants at 450 K are stronger bounded around the pole and are mixed more intensively than the remnants at 585 K.

Before we quantify these properties more precisely, some remarks on the validity of the isentropic calculations are necessary. The isentropic approximation is motivated by weak diabatic descent of the vortex air at both levels during the considered periods. Figure 2 shows the averaged descent of an ensemble of trajectories starting in vortex or, if vortex is not present, in the regions of sufficiently high PV values calculated between September 1999 and Mai 2000. The diabatic descent rates are derived from the radiation module (Zhong and Haigh, 1995) based on the Morcrette scheme (Morcrette, 1991). Thus, between mid-February and the end of May, the potential temperature θ of the vortex air masses does not significantly change in the θ-range between 400 and 600 K.

Aditionally, we verify the quality of the CLaMS transport by comparing the simulated distributions of CH_4 with the HALOE observations. Figure 3 shows the results of such comparison for two CLaMS configurations: without mixing (i.e. transport only in terms of forward trajectories) and with the adjusted mixing. The correlation coefficient ρ between the observed and simulated mixing ratios (see legend in Fig. 3) show that the CLaMS simulation with adjusted mixing reproduces fairly well the CH_4-distributions observed by HALOE in spring and summer 1997 northward of 30° N. Furthermore, the CLaMS mixing scheme smoothes out some of the very low CH_4 mixing ratios present in the pure advection transport that are not observed by HALOE (in particular at 585 K). Consequently, the correlation coefficient ρ between the HALOE observations and CLaMS simulations increases from 0.5 to 0.74 and from 0.38 to 0.64 for θ = 450 and 585 K, respectively. The deviations still present at 585 K are mainly caused by the errors of the simulated absolute position of the vortex remnants. This indicates that the quality of the ECMWF winds is better at 450 than at 585 K.

Thus, using 3d-trajectory calculations and by comparing CLaMS CH_4-distributions with the HALOE observations, we conclude that isentropic transport dominated the propagation of the vortex air into the mid-latitudes several weeks before and after breakup of the vortex in 1997 and 2000.

3. Spatial distribution and lifetime of vortex remnants in 1997 and 2000

In 1997, the polar vortex was unusually long lived (Coy et al., 1997). Even at the end of April, the vortex was very symmetric around the pole and stable, and it did not breakup until mid of May. On the other hand, the breakup of the vortex in 2000 was around mid of March, i.e. during a time period typical for the onset of the final warming in the northern hemisphere (Manney and Sabutis, 2000).

The zonal distribution of the vortex remnants after the vortex breakup is mainly determined by the isentropic winds. In Fig. 4 the zonal mean winds at 450 and 585 K are shown for both considered periods. Owing to the long vortex lifetime in 1997, the vortex breakup at 585 K is accompanied by a transition from the winter to the summer circulation with no influence of the subtropical jet. On the other hand, the transport of vortex remnants at 450 K, is driven by westerly winds and influenced by the subtropical jet. The zonally averaged winds in 2000 show a similar structure although a strong subtropical jet is present even in the upper level and the summer circulation is still not fully developed owing to the earlier breakup time.

By performing the CLaMS simulations, we investigate now the meridional distribution of the vortex air and the influence of mixing (i.e. of the irreversible part of transport) on a such distribution. CLaMS results for the zonally averaged meridional distribution of the vortex air after the vortex breakup in 1997 are shown in Fig. 5. Results at 450 K (left) and 585 K (right) are plotted for tracer transport without mixing (top) and with an excessive mixing (bottom) corresponding to the mean distance between neighboring APs $r_0 = 200$ km. In the model, vortex air is defined as air masses bounded at the beginning of the simulation by the vortex edge identified by the strongest PV gradient with respect to equivalent latitude (Nash et al., 1996). To mark vortex air, an additional, artificial tracer is used and initialized as 1 and 0 within and outside of the vortex, respectively. The subsequent transport (advection + mixing) of this tracer describes the zonal distribution of the vortex air.

The comparison between top and bottom panels of Fig. 5 shows a negligible influence of mixing on the zonal distribution of the vortex air. Even for CLaMS simulations without mixing, the zonal averaging of the (unmixed) air parcels leads to a similar meridional distribution of the vortex air as in the case where mixing was exaggerated. Thus, the large scale meridional transport of vortex air into the mid-latitudes is dominated by the chaotic advection (induced e.g. by planetary waves) rather than by mixing. The zonally averaged tracks of vortex remnants (black lines in Figs. 5 and 4) show at 585 K a stronger southward propagation than at 450 K. In agreement with the investigations of Piani et al. (2002a), this propagation at 450 K is confined by the subtropical jet to latitudes poleward of 55° N. The southward transport of vortex air at 585 K is more effective and reaches about 40° N.

However, mixing may significantly influence the lifetime of vortex remnants, i.e., the time that is necessary to homogeneously mix vortex air with ambient air. The temporally and spatially inhomogeneous CLaMS mixing is driven by integral flow deformation that can be quantified in terms of the finite-time Lyapunov exponent λ . Thus, CLaMS produces high mixing intensity only in flow regions with sufficiently high values of λ. Figure 6 shows the zonally averaged Lyapunov exponents λ calculated for each CLaMS AP over a time step $\Delta t = 12$ h. After the vortex breakup, the summer circulation at 585 K is characterized by very low values of λ. Generally, the summer circulation in the middle stratosphere can be understood as a “solid body rotation” with a negligible amount of local strain between the neighboring APs (Piani et al., 2002b). Consequently, the regridding algorithm in CLaMS that is driven by the local deformation rates, indicates very weak mixing at this level.

To quantify the effect of mixing on the lifetime of vortex remnants the PDFs (probability density function) calculated for CLaMS CH_4 distributions are shown in Fig. 7. The

PDF is proportional to the area occupied by tracer values in a given range of mixing ratios (for details see e.g. Sparling, 2000). Here, the black lines denote the vortex edge transformed from the PV to CH_4-field. Thus, the PDF of the CH_4-values below these lines describe the contribution of vortex air to all air masses poleward of 30° N. The results show that the vortex remnants disappear significantly faster at 450 than at 585 K. The greater Lyapunov exponents in the lower level cause more stirring, greater local deformation rates, and, consequently, more mixing. The lifetime of the vortex remnants at 450 and 585 K is of the order 5 and 10 weeks, respectively. The behavior of vortex remnants formed in March 2000 is similar but, due to an earlier vortex breakup, dominated until mid of May by westerly winds, even at 585 K.

It should be emphasized that isentropic simulations may overestimate the lifetime of the vortex remnants, especially in the last phase of their existence when the remnants are losing their vertical coherence. Here, the vortex fragments may form elongated and slanted sheets of air, the so-called laminae (see e.g. Orsolini et al., 1995) with a very complicated contact surface separating the vortex from the mid latitude air (Haynes and Anglade, 1997). Thus, although the isentropic 2d simulations underestimate such contact surfaces and, consequently, overestimate the lifetime of the vortex remnants, the ratio of their lifetimes is a rather reliable quantity. We conclude that the lifetime of the remnants at 585 K is by a factor of 2 longer than at 450 K.

4. Ozone chemistry in vortex remnants

In the previous section, we have shown that the vortex air trapped in the long-lived vortex remnants is well-isolated from the mid-latitudes. Here, we discuss some properties of the O_3-chemistry observed and simulated in such remnants in spring/summer 1997 and 2000. It is a well-established fact that the Arctic O_3 loss is due to halogen-catalyzed ozone loss with primary contributions of the reactive chlorine and bromine species which are activated heterogeneously on the surface of the polar stratospheric cloud particles, a primary component of which is nitric acid (HNO_3) (Solomon, 1999).

Under Arctic conditions, the ozone loss terminates in spring, as chlorine is deactivated through the formation of $ClONO_2$ and a subsequent transformation to HCl (Douglass et al., 1995). The main source of NO_x that is controlling the deactivation of ClO_x is either the photolysis of HNO_3, its reaction with OH, or its flux from mid-latitudes. During the period when $ClONO_2$ is converted into HCl, the photolytically or heterogenously induced reactivation of ClO_x from $ClONO_2$ is still possible.

Thus on the one hand, the formation of HCl in the vortex air determines when the chlorine-induced O_3-destruction is terminated. On the other hand, the breakup of the vortex defines when chaotic advection and intense mixing dominate the transport of vortex air into the mid-latitudes. Figure 8 shows the simulated HCl distributions (using the adjusted mixing) two days after the vortex breakup in 1997 and 2000. The black circles denote the corresponding HALOE observations that in the vortex remnants agree fairly well with the CLaMS calculations. The high HCl mixing ratios that were observed in May 1997 indicate a completed chlorine deactivation whereas this process is still under way in March 2000. As can be seen in Fig. 9, first at the end of April (i.e. 44 days after the vortex breakup) significantly enhenced mixing ratios of HCl become apparent in the simulated vortex remnants that were also observed by HALOE (Müller et al., 2002).

A more quantitative description of the deactivation process is given in Fig. 10 where the mean O_3-loss rate (per day) averaged over the vortex air together with the partitioning of O_3-loss into different chemical destruction cycles are shown. To distinguish the vortex from the mid-latitude air, we use the transported (i.e. advected and mixed) PV fields. Then, the vortex air is defined as air masses with PV values larger than PV at the vortex edge (Nash et al., 1996) at the beginning of the simulation.

A comparison of the mean net O_3-loss rate at 450 K during the time periods around the vortex breakup in 1997 and 2000 shows in March 2000 significantly more O_3-depletion than in May 1997. In particular, between the time of the vortex breakup around mid-March and mid-April 2000, the O_3 destruction in the vortex remnants was still dominated by the halogen cycles (green line). By contrast, in mid-May 1997, these cycles are negligible, even shortly before the vortex breakup. As already mentioned, these differences can be explained by the fact that the chlorine deactivation due to formation of HCl is completed before the final vortex breakup in May 1997, whereas the formation of HCl in spring 2000 is finished in the vortex remnants in mid-April.

At 450 K the contribution of HO_x (HO_x=HO_2+OH) outweights the NO_x-induced ozone destruction and is dominated by the direct reaction of HO_x with ozone. Here, the ozone destruction driven by NO_x that was formed by photolytical decomposition of $ClONO_2$ (Toumi et al., 1993) is classified as NO_x-induced ozone destruction and contributes up to 45% to the NO_x-cycles around mid of April (not shown in Fig. 10).

A similar analysis of the O_3-chemistry in the long-lived vortex remnants at 585 K in 1997 shows that the most important destruction cycle is the "summertime" NO_x-chemistry (Hansen and Chipperfield, 1999; Fahey and Ravishankara, 1999). Furthermore, the fractional contribution of the different cycles to the O_3-loss in the vortex remnants does not significantly differ from the O_3-loss partitioning calculated for extra-vortex air masses northward of 60° N (not shown). So although the chemical composition of the coarsely-mixed vortex remnants still differs from the composition of the ambient air, the contribution of the O_3-loss cycles to the total O_3-depletion is very similar in both types of air.

The fact that deactivation process in spring 1997 was still completed in a well-isolated vortex indicates that at least in this year, the chlorine deactivation was decoupled from mixing and mainly driven by the in situ chemical production of NO_x. On the other side, the incomplete deactivation shortly before the vortex breakup in March 2000 offers the possibility to study the influence of mixing on this process during the final vortex decay.

5. The impact of mixing

Using different values of the mixing parameters, we now study the influence of mixing on the accumulated ozone loss in the mid and high latitudes after the vortex breakup around mid-March 2000 at the isentropic surface 450 K. The accumulated ozone loss is defined as the difference between the passively transported and chemically changed ozone. Here, this difference is determined for the time period between 10.02 and 31.05.2000 and averaged over all air masses poleward of 30° N. The results calculated for the adjusted mixing are shown in Fig. 11 (red line).

In order to study the influence of halogen chemistry on the O_3-loss, the black line describes the accumulated ozone loss calculated from a chemistry run without halogen cycles (Cl_y=Br_y=0). The yellow curve describes the accumulated ozone loss for a scenario with a strong denitrification as would be expected for Antarctic conditions (HNO_3≈2 ppbv in the vortex). The remaining curves describe the sensitivity of the reference simulation (red) on the intensity of mixing with effective diffusivity varying between 1.1 10^3 and 4.2 10^5 m^2s^{-1}

Thus, the mid-latitude ozone deficit in spring 2000, defined here as the difference between the red and black curves, can be divided into 3 phases (see dashed red lines in Fig. 11): Until mid-March ozone destruction due to halogen chemistry occurs in a well-isolated Arctic vortex. From mid-March (vortex breakup) until mid-April the ozone-depleted air masses are transported into the mid-latitudes. By comparing the slopes of the red and black lines during this period, we conclude that the chlorine and bromine chemistry still destroy ozone in vortex remnants (see Fig. 10), albeit with a smaller intensity than in February and in early March. Here, the main source of active chlorine is the photolysis of $ClONO_2$. Between mid-April and end of May, the slopes of the dashed black and red lines are comparable and, consequently, the halogen-induced ozone destruction is negligible during this period. Thus, compared with the ozone distribution in a halogen-free stratosphere (black line), the mid-latitude ozone deficit at isentropic level 450 K can be determined. Thus, the chlorine-induced ozone deficit amounts end of May 2000 to about 12%. The contribution of the vortex remnants formed after the vortex breakup can be quantified by about 2%.

The sensitivity studies with respect to mixing show that the accumulated ozone loss does not change as long as the effective diffusivity in the model is smaller than 3×10^4 m^2/s. This value corresponds to a spatial resolution of the order 100 km. Also, the deactivation of ClO_x via formation of $ClONO_2$ is mainly due to photochemical decomposition of HNO_3 rather than due to chemistry induced by mixing of the activated vortex air with NO_x-rich mid-latitude air. Only for the diffusion being greater than an unrealistically large critical value of 10^5 m^2/s (corresponding to a spatial resolution of the order 200 km) mixing of mid-latitude air has a significant impact on $ClONO_2$ formation in vortex remnants.

Using an Eulerian model, Tan et al. (1998) postulated a much stronger influence of the numerical mixing on the chlorine deactivation. They concluded that Eulerian grid resolution better than 40 km is necessary to correctly describe the deactivation process. Assuming that the numerical diffusivity is proportional to $r_0^2/\Delta t$ than the discussed Lagrangian critical resolution $r_{0L} = r_0 \approx 100$ km can be transformed to an equivalent Eulerian resolution r_{0E} by $r_{0E} = r_{0L}\sqrt{\Delta t_E/\Delta t_L}$ where $\Delta t_L \approx 24$ h and $\Delta t_E \approx 15$ min are the typical Lagrangian and Eulerian time steps. Using this crude estimate, we obtain $r_{0E} \approx 10$ km that probably underestimates the critical resolution of the Eulerian schemes discussed by Tan et al. (1998). Nevertheless, the small numerical diffusion of the Lagrangian transport allows to study the mixing-sensitive processes by using model resolutions that are coarser than the corresponding Eulerian studies.

In addition, our studies show that mixing may influence chemistry in some small-scale filaments during their final dissipation. For budget studies (e.g. impact of mixing on the mid-latitude ozone deficit) such small-scale structures are negligible if compared with large, coherent vortex fragments where the bulk contribution outweights the effect of the mixing-sensitive surface. Thus, even after the vortex breakup in mid-March 2000, the averaged deactivation process is dominated by in situ chemistry rather than mixing. Furthermore, the results of pure advection studies (i.e. in terms of the photochemical box model) do not significantly differ from the simulations with the adjusted mixing. One reason for this weak impact of mixing on the O_3-chemistry may be the fact that shortly before the vortex breakup a significant amount of active chlorine was still transformed into $ClONO_2$. If strong intrusions of the mid-latitude air occur into a vortex with chlorine fully activated (as discussed e.g. in Plumb et al., 1994), the importance of mixing on the deactivation process may be higher.

6. Conclusions

Full chemistry simulations were carried out with the Chemical Lagrangian Model of the Stratosphere (CLaMS) to study the spatial distribution, lifetime and O_3-chemistry of the vortex remnants created after the vortex breakup in spring and summer 1997 and 2000. Isentropic 2d simulations on two isentropic levels 450 K (≈18 km) and 585 K (≈24 km) have been conducted with a very high spatial resolution (up to 20 km) in order to resolve the filamentary structure of slowly dissipating vortex remnants. The isentropic approximation was justified by the comparison with the HALOE tracer measurements and radiation calculations.

In agreement with the investigations of Orsolini (2001) and Piani et al. (2002a), the zonal distribution of the vortex air after the vortex breakup shows different patterns above and belove 20 km. Especially in summer 1997 the differences are evident with long-lived vortex remnants above 20 km, which are trapped in the "solid body" summer circulation, and, below 20 km, with a significant stirring and mixing caused by the influence of the subtropical jet. The subtropical jet bounds the southward propagation of the remnants up to 55° N whereas above 20 km a coarsely-mixed vortex air may reach 40° N. Although the meridional distribution of such remnants is mainly determined by the chaotic advection, their lifetime, in contrast, strongly depends on mixing and above 20 km it is approximately twice as long as below 20 km. The isentropic simulations may underestimate mixing and, consequently, the absolute lifetimes of the vortex remnants, in particular, during the phase when the vortex remnants loose their vertical coherence.

The different times of vortex breakup in 1997 and 2000 are responsible for different chemical signatures in vortex remnants simulated with CLaMS and observed by HALOE. The O_3-chemistry in the vortex remnants strongly depends on the partitioning between active and reservoir compounds within the Cl_y and Br_y families. If shortly before the vortex breakup, most of the chlorine is contained in HCl (as in 1997) then small ozone loss rates have to be expected in the vortex remnants which are mainly driven by the HO_x (450 K) and NO_x (585 K) destruction cycles. If, on the other hand, $ClONO_2$ and partially ClO_x are the main reservoirs of the chlorine shortly before the vortex breakup (as in 2000), then a chlorine-induced ozone destruction within the vortex remnants can be expected mainly due the photolytical decomposition of $ClONO_2$. The impact of mixing is negligible due to a negligible flux of NO_x into the (coherent) vortex remnants. Here, the more important source of NO_x is the photolytical decomposition of HNO_3.

For both investigated periods the simulated O_3-loss in the vortex remnants is dominated by the in situ chemistry in the Lagrangian air parcels rather than by mixing between these air parcels and the mid-latitude air. The sensitivity studies with respect to mixing show that the accumulated ozone loss does not change as long as the effective diffusivity in the model is smaller than 10^4 m^2/s that is if the (Lagrangian) model resolution is better than 100 km.

Acknowledgements. The European Centre for Medium-Range Weather Forecasts (ECMWF) and the United Kingdom Meteorological Office (UKMO) are acknowledged for meteorological data support. This work was funded by the European Union under the contract number EVK2-1999-00311 (EU THESEO 2000) and EVK2-CT-1999-000049 (SAMMOA).

References

Balluch, M. G. and Haynes, P. H.: Quantification of lower stratospheric mixing processes using aircraft data, J. Geophys. Res., 102, 23 487–23 504, 1997. 1054

Chipperfield, M. P. and Jones, R. L.: Relative influences of atmospheric chemistry and transport on arctic ozone trends, Nature, 400, 551–554, 1999. 1053

Coy, L., Nash, E., and Newman, P.: Meteorology of the polar vortex: Spring 1997, Geophys. Res. Lett., 24, 2693–2696, 1997. 1055, 1058

Douglass, A. R., Schoeberl, M. R., Stolarski, R. S., Waters, J. W., Russell III, J. M., Roche, A. E., and Massie, S. T.: Interhemispheric differences in springtime production of HCl and $ClONO_2$ in the polar vortices, J. Geophys. Res., 100, 13 967–13 978, 1995. 1061

Title Page
Abstract | Introduction
Conclusions | References
Tables | Figures
◀| |▶
◀ ▶
Back | Close
Full Screen / Esc
Print Version
Interactive Discussion

Edouard, S., Legras, B., Lefèvre, F., and Eymard, R.: The effect of small-scale inhomogeneities on ozone depletion in the Arctic, Nature, 384, 444–447, 1996. 1054

Fahey, D. and Ravishankara, A.: Summer in the stratosphere, Science, 285, 208–210, 1999. 1062

Grooß, J.-U., Günther, G., Konopka, P., Müller, R., McKenna, D. S., Stroh, F., Vogel, B., Engel, A., Müller, M., Hoppel, K., Bevilacqua, R., Richard, E., Webster, C. R., Elkins, J. W., Hurst, D., Romashkin, P. A., and Baumgardner, D. G.: Simulation of ozone depletion in spring 2000 with the Chemical Lagrangian Model of the Stratosphere (CLaMS), J. Geophys. Res., 107, 8295, doi:10.1029/2001JD000 456, 2002. 1057

Hansen, G. and Chipperfield, M. P.: Ozone depletion at the edge of the Arctic polar vortex 1996/1997, J. Geophys. Res., 104, 1837–1845, 1999. 1062

Haynes, P. and Anglade, J.: The vertical scale cascade in atmospheric tracers due to large-scale differential advection, J. Atmos. Sci., 54, 1121–1136, 1997. 1060

Hess, P.: Mixing processes following the final stratospheric warming, J. Atmos. Sci., 42, 1625–1641, 1991. 1053

Knudsen, B. M. and Grooß, J. U.: Northern midlatitude stratospheric ozone dilution in spring modeled with simulated mixing, J. Geophys. Res., 105, 6885 – 6890, 2000. 1053

Konopka, P., Grooß, J. U., Günther, G., McKenna, D. S., Müller, R., Elkins, J. W., Fahey, D., Popp, P., and Stimpfle, R. M.: Weak influence of mixing on the chlorine deactivation during SOLVE/THESEO2000: Lagrangian modeling (CLaMS) versus ER-2 in situ observations, J. Geophys. Res., 108, D5, 10.1029/2001JD00876, 2003. 1056, 1057

Manney, G. L. and Sabutis, J. L.: Development of the polar vortex in the 1999-2000 Arctic winter stratosphere, Geophys. Res. Lett., 27, 2589–2592, 2000. 1055, 1058

Marchand, M., Godin, S., Hauchecorne, A., Lefèvre, F., and Bekki, S.: Influence of polar ozone loss on Northern mid-latitude regions estimated by a high resolution chemistry transport model during winter 1999–2000, J. Geophys. Res., 108, D5, 10.1029/2001JD000906, 2003. 1054

McKenna, D. S., Grooß, J.-U., Günther, G., Konopka, P., Müller, R., Carver, G., and Sasano, Y.: A new Chemical Lagrangian Model of the Stratosphere (CLaMS): Part II Formulation of chemistry-scheme and initialisation, J. Geophys. Res., 107, 10.1029/2000JD000 113, 2002a. 1054

McKenna, D. S., Konopka, P., Grooß, J.-U., Günther, G., Müller, R., Spang, R., Offermann, D., and Orsolini, Y.: A new Chemical Lagrangian Model of the Stratosphere (CLaMS): Part I Formulation of advection and mixing, J. Geophys. Res., 107, 10.1029/2000JD000 114, 2002b. 1054, 1056

Morcrette, J.-J.: Radiation and cloud radiative properties in the European Centre for Medium-Range Weather Forecasts forecasting system, J. Geophys. Res., 96, 9121–9132, 1991. 1057

Müller, R., Tilmes, S., Grooß, J.-U., McKenna, D. S., Müller, M., Schmidt, U., Toon, G. C., Stachnik, R. A., Margitan, J. J., Elkins, J. W., Arvelius, J., and III, J. M. R.: Chlorine activation and chemical ozone loss deduced from HALOE and balloon measurements in the Arctic during the winter of 1999-2000, J. Geophys. Res., 107, 8302, doi:10.1029/2001JD001 423, 2002. 1061

Nash, E. R., Newman, P. A., Rosenfield, J. E., and Schoeberl, M. R.: An objective determination of the polar vortex using Ertel's potential vorticity, J. Geophys. Res., 101, 9471–9478, 1996. 1059, 1061, 1076

Orsolini, Y., Simon, P., and Cariolle, D.: Filamentation and layering of an idealized tracer by observed winds in the lower stratosphere, Geophys. Res. Lett., 22, 839–842, 1995. 1060

Orsolini, Y. J.: Long-lived tracer patterns in the summer polar stratosphere, Geophys. Res. Lett., 28, 3855–3858, 2001. 1053, 1065

Orsolini, Y. J., Hansen, G., Hoppe, U. P., Manney, G. L., and Fricke, K. H.: Dynamical modelling of wintertime lidar observations in the Arctic, Q. J. R. Meteorol. Soc., 123, 785–800, 1997. 1054

Piani, C., Norton, W. A., Iwi, A. M., Ray, E. A., and Elkins, J. W.: Transport of ozone-depleted air on the breakup of the stratospheric polar vortex in spring/summer 2000, J. Geophys. Res., 107, D20, 10.1029/2001JD00488, 2001. 1053, 1059, 1065

Piani, C., Norton, W. A., and Swindley, S.: Solid-body rotation in the northern summer stratosphere, Geophys. Res. Lett., 29, 23, 10.1029/2002GL016079, 2002b. 1059

Plumb, R. A., Waugh, D. W., Atkinson, R. J., Newman, P. A., Lait, L. R., Schoeberl, M. R., Browell, E. V., Simmons, A. J., and Loewenstein, M.: Intrusions into the lower stratospheric Arctic vortex during the winter of 1991-1992, J. Geophys. Res., 99, 1089–1105, 1994. 1054, 1064

Riese, M., Tie, X., Brasseur, G., and Offermann, D.: Three-dimensional simulation of stratospheric trace gas distributions measured by CRISTA, J. Geophys. Res., 104, 16 419–16 435, 1999. 1054

Searle, K. R., Chipperfield, M. P., Bekki, S., and Pyle, J. A.: The impact of spatial averaging on calculated polar ozone loss: I. Model experiments, J. Geophys. Res., 103, 25 397–25 408, 1998a. 1054

Searle, K. R., Chipperfield, M. P., Bekki, S., and Pyle, J. A.: The impact of spatial averaging on calculated polar ozone loss: II. Theoretical analysis, J. Geophys. Res., 103, 25 409–25 416, 1998b. 1054

Solomon, S.: Stratospheric ozone depletion: A review of concepts and history, Rev. of Geophys., 37, 275–316, 1999. 1060

Sparling, L. C.: Statistical perspectives on stratospheric transport, Rev. Geophys., 38, 417–436, 2000. 1060

Tan, D. G. H., Haynes, P. H., MacKenzie, A. R., and Pyle, J. A.: Effects of fluid-dynamical stirring and mixing on the deactivation of stratospheric chlorine, J. Geophys. Res., 103, 1585–1605, 1998. 1054, 1064

Toumi, R., Jones, R. L., and Pyle, J. A.: Stratospheric ozone depletion by $ClONO_2$ photolysis, Nature, 365, 37–39, 1993. 1062

Tuck, A. F.: Synoptic and chemical evolution of the Antarctic vortex in late winter and early spring, 1987, J. Geophys. Res., 94, 11 687–11 737, 1989. 1054

Waugh, D. W., Plumb, R. A., Elkins, J. W., Fahey, D. W., Boering, K. A., Dutton, G. S., Volk, C. M., Keim, E., Gao, R.-S., Daube, B. C., Wofsy, S. C., Loewenstein, M., Podolske, J. R., Chan, K. R., Proffitt, M. H., Kelly, K. K., Newman, P. A., and Lait, L. R.: Mixing of polar vortex air into middle latitudes as revealed by tracer-tracer scatterplots, J. Geophys. Res., 102, 13 119–13 134, 1997. 1054

WMO: Scientific assessment of ozone depletion: 1998, Report No. 44, Geneva, 1998. 1053

Zhong, W. and Haigh, J. D.: Improved broadband emissivity parameterization for water vapor cooling rate calculations, J. Atmos. Sci., 52, 124–138, 1995. 1057

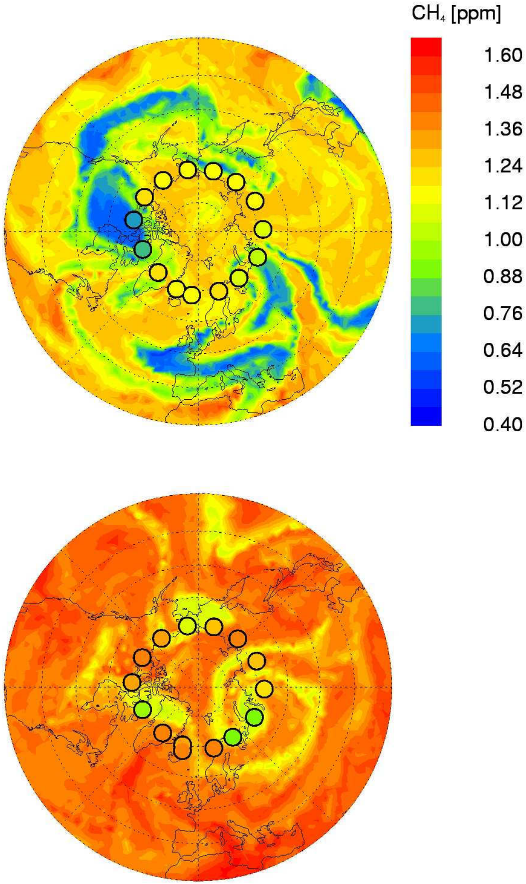

Fig. 1. CH_4 simulated with CLaMS at θ = 585 K (top) and 450 K (bottom) at 22 May 1997, i.e. about 12 days after the vortex breakup. The circles denote the HALOE observations mapped to the same synoptic time.

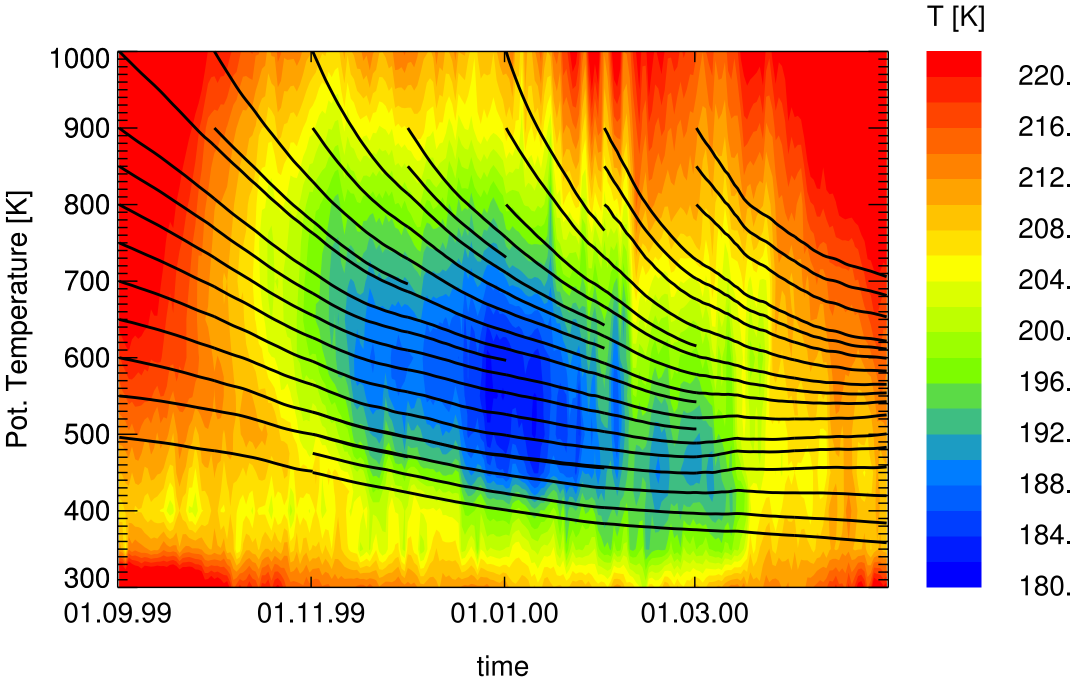

Fig. 2. Averaged diabatic descent of an ensemble of trajectories (black lines) starting in the vortex in September 1999. The colors describe the minimum temperature in the vortex during the considered period. The potential temperature of the vortex air masses does not significantly change between mid-February and the end of May in the θ-range between 400 and 600 K.

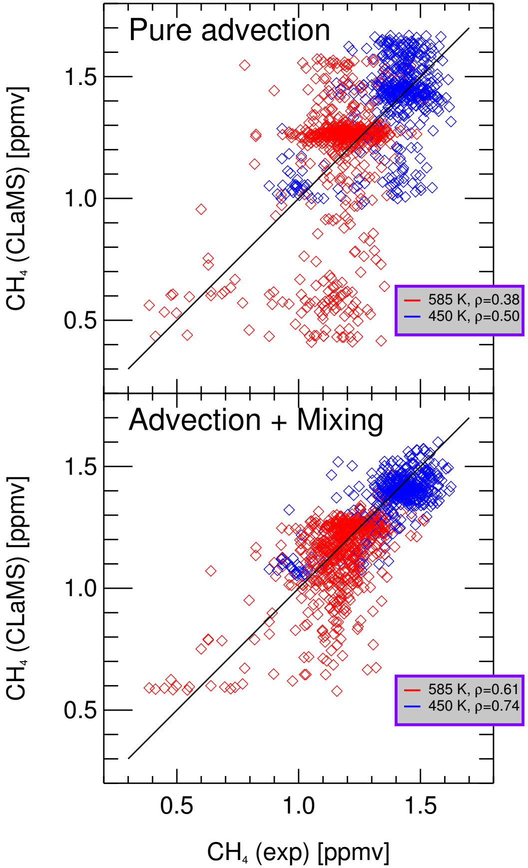

Fig. 3. CLaMS transport of CH_4 versus HALOE observations northward of 30° N between 10 April and 31 June 1997 at θ = 450 and θ = 585 K without mixing (upper panel) and with adjusted mixing (lower panel).

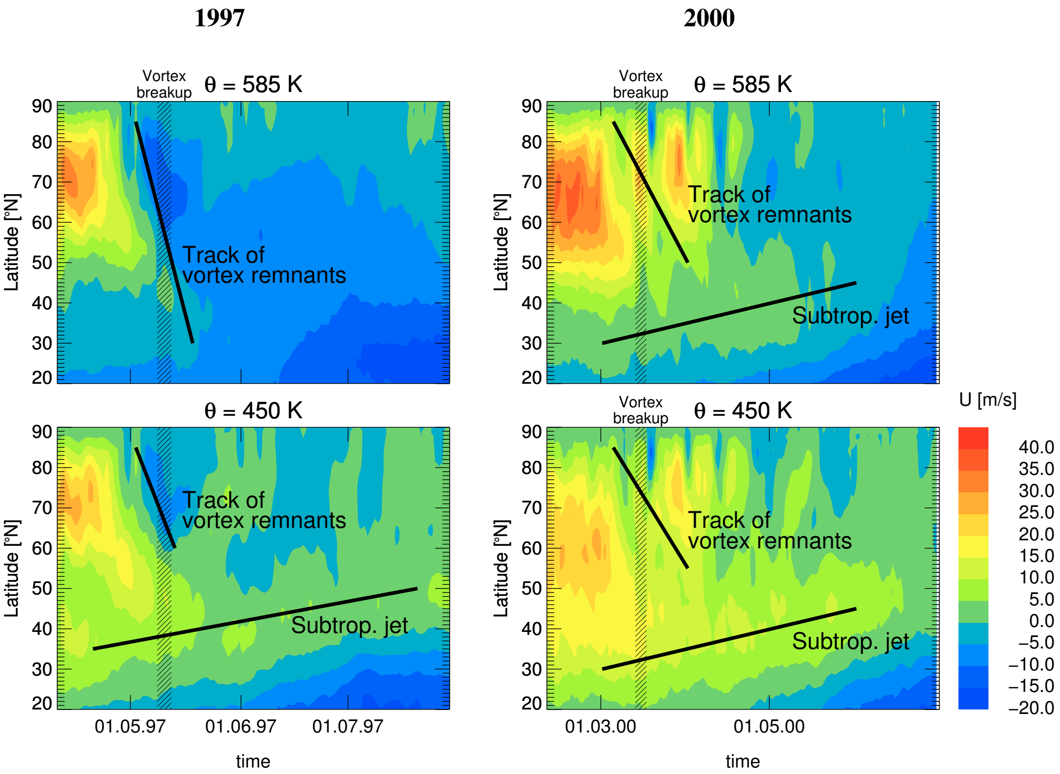

Fig. 4. Zonal mean ECMWF winds at $\theta = 450$ (bottom panels) and 585 K (top panels) for the 1997 (left) and 2000 (right) period. The southward propagation of the vortex remnants is bounded by the subtropical jet. Their meridional tracks are derived from zonally averaged distribution of the vortex air (see Fig. 5).

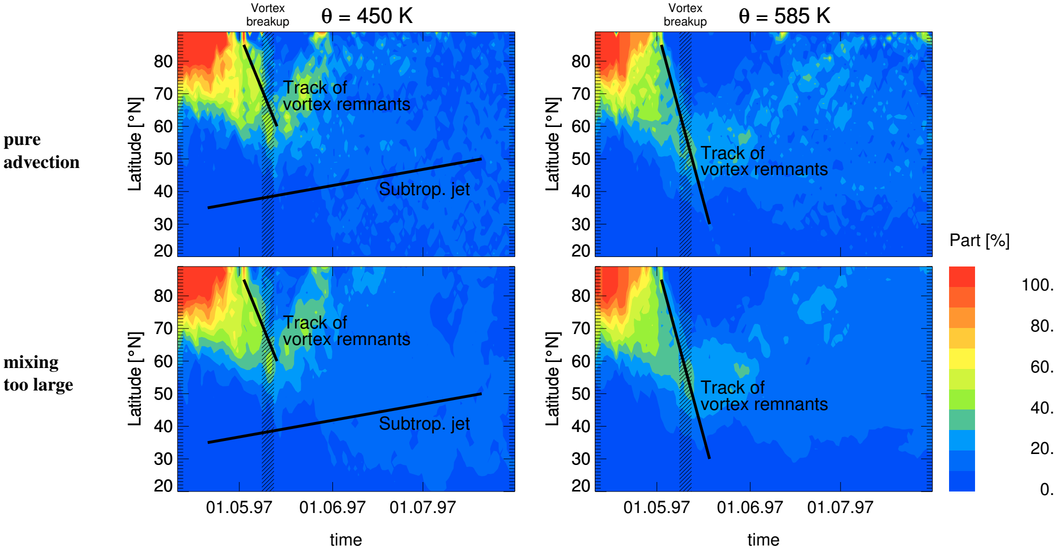

Fig. 5. Meridional (zonally averaged) contribution of vortex air at θ = 450 (left) and 585 K (right) for CLaMS simulation without (top) and with excessive (bottom) mixing. The colors denote the zonally averaged rate the vortex air changing from 100% (pure vortex air) to 0% (pure extra vortex air). The black lines denote the tracks of the vortex air masses during their transport into the mid latitudes (see also Fig. 4).

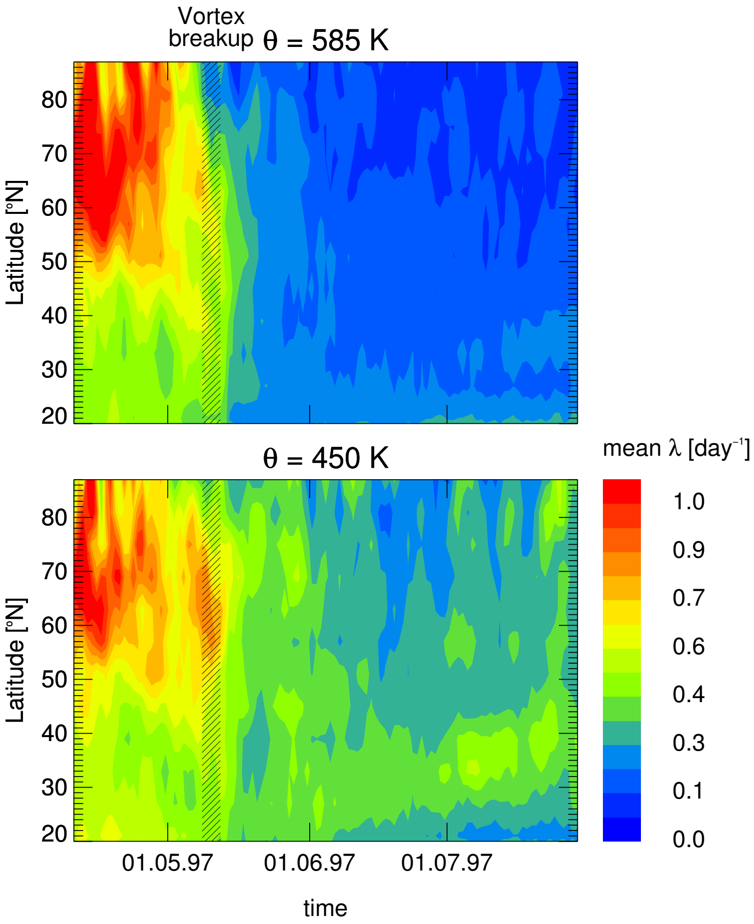

Fig. 6. Zonally averaged Lyapunov exponent λ during the 1997 period calculated over a time step $\Delta t = 12$ h at $\theta = 450$ and 585 K. Note that the summer circulation at 585 K is characterized by very low values of λ.

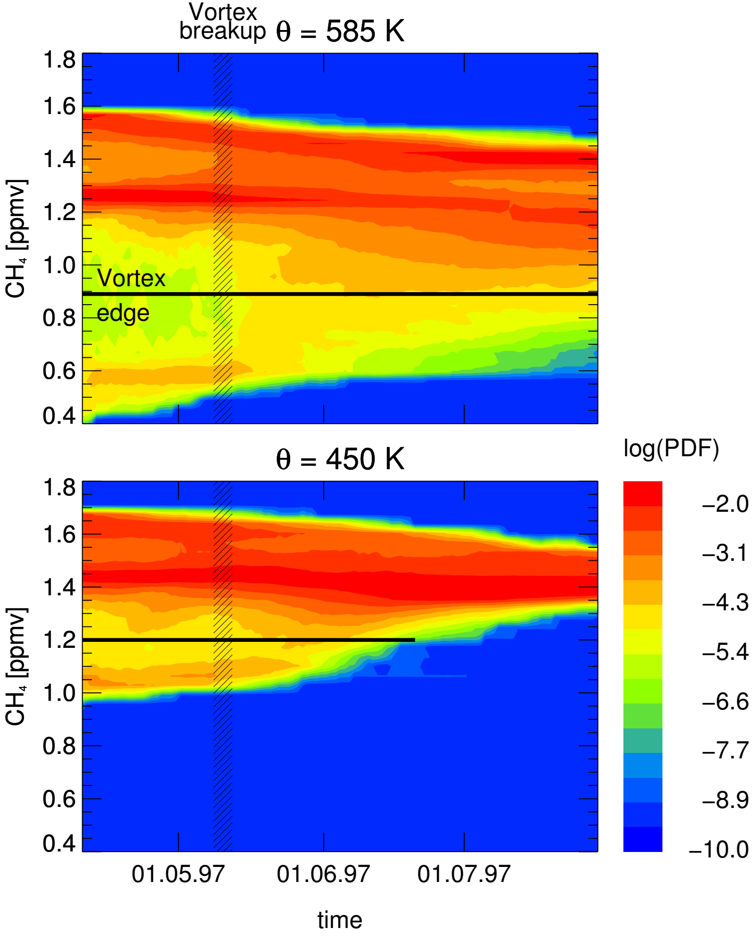

Fig. 7. PDF of CH_4 at θ = 450 and 585 K. The black lines denote the mean CH_4 at the vortex edge at the beginning of the simulation. The vortex edge was determined by using the Nash criterion (Nash et al., 1996).

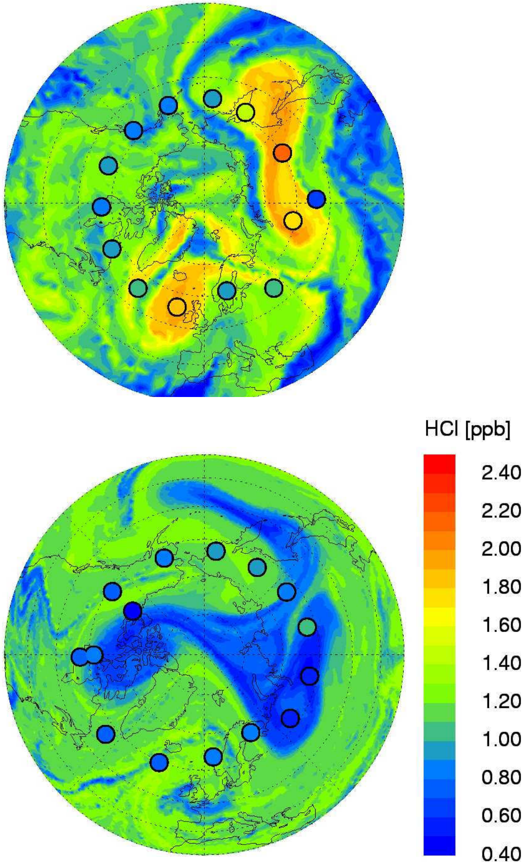

Fig. 8. HCl simulated with CLaMS at θ = 450 K 2 days after the vortex breakup at 12 May 1997 (top) and 17 March 2000 (bottom). High values of HCl indicate a completed chlorine deactivation. The circles denote the HALOE observations.

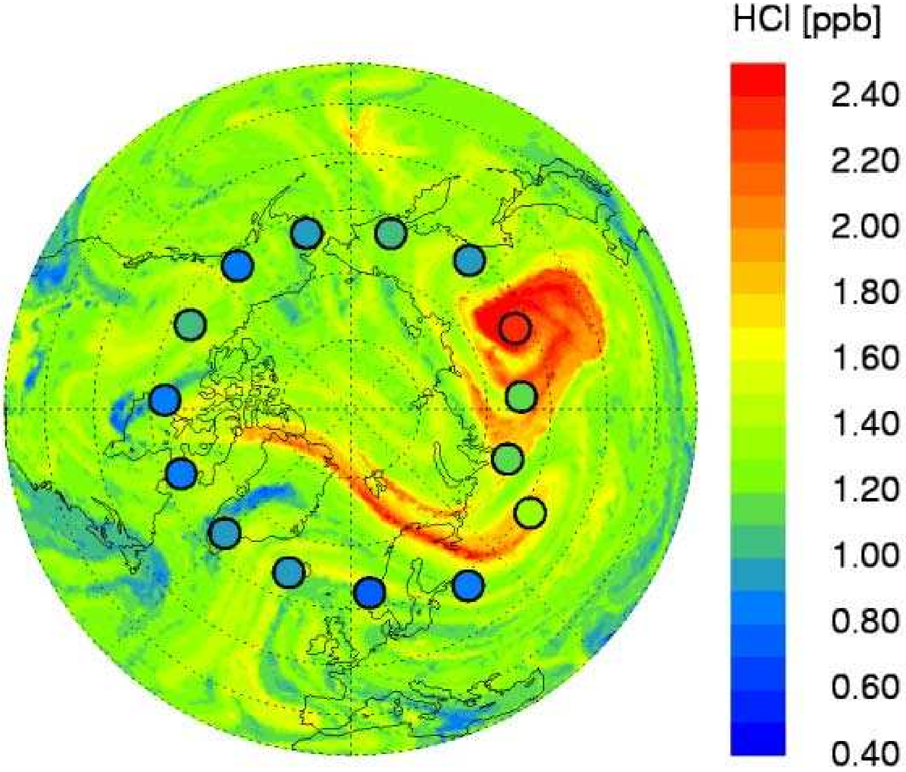

Fig. 9. HCl simulated with CLaMS at θ = 450 K on 29 April 2000, i.e. 44 days after the vortex breakup.

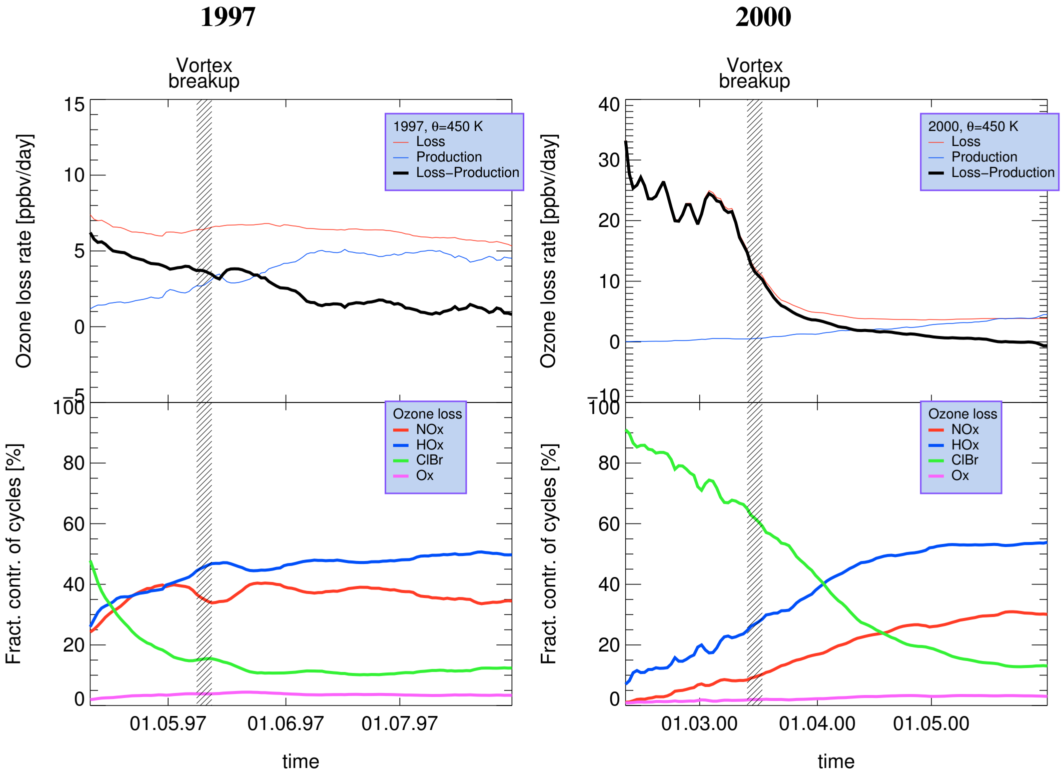

Fig. 10. Top: Mean ozone loss rate (per day) in the vortex air (i.e. air masses with transported PV larger than vortex edge PV at the beginnig of the simulation). Bottom: Contribution of different chemical destruction cycles at 450 K in 1997 (left) and 2000 (right).

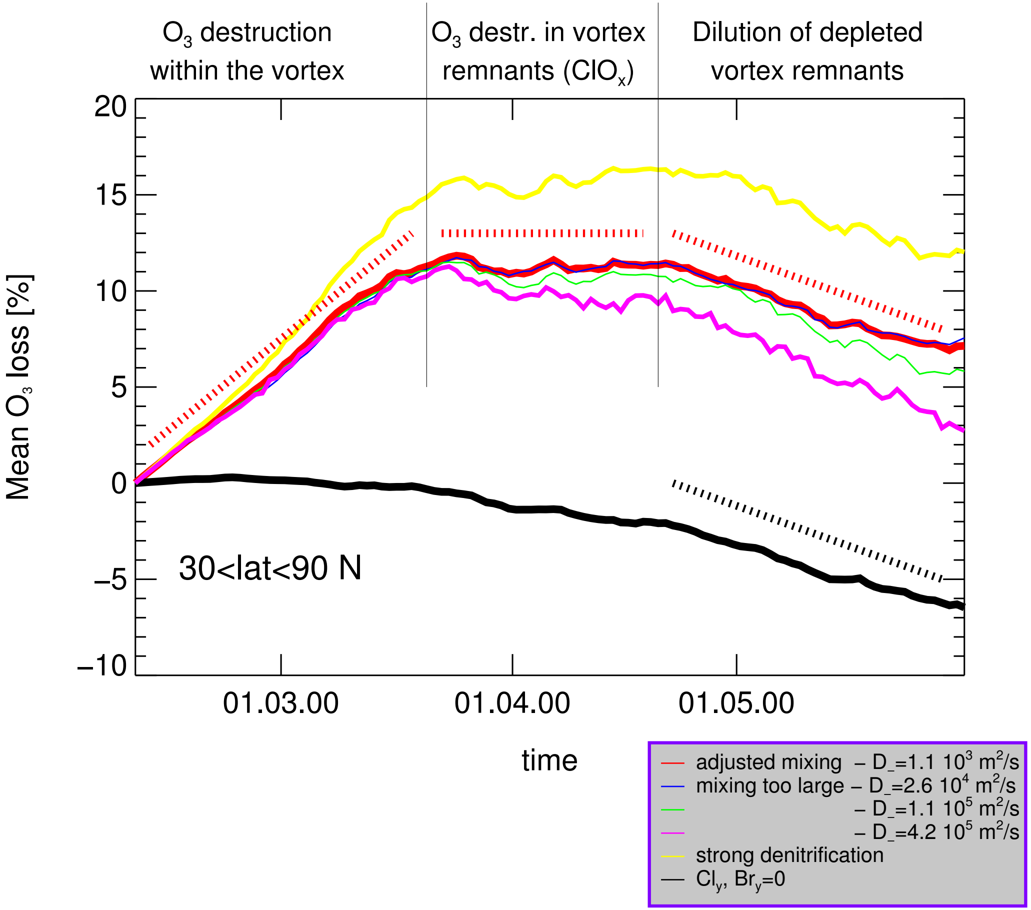

Fig. 11. Accumulated ozone loss poleward of 30° N at 450 K.

Title Page
Abstract | Introduction
Conclusions | References
Tables | Figures
◀| |▶
◀ ▶
Back | Close
Full Screen / Esc
Print Version
Interactive Discussion